

# PARTIALLY PARALLEL MR IMAGE RECONSTRUCTION USING SENSITIVITY ENCODING \*

Maryam Yashtini, William W. Hager, Yunmei Chen

Xiaoqing Ye

University of Florida  
Department of Mathematics  
Gainesville, FL

Georgia Institute of Technology  
Department of Mathematics  
Atlanta, GA

## ABSTRACT

A new algorithm is presented for efficiently solving image reconstruction problems that arise in partially parallel magnetic resonance imaging. This algorithm minimizes an objective function of the form  $\phi(Bu) + \frac{1}{2}\|\mathcal{F}_p Su - f\|^2$ , where  $\phi$  is the regularization term which may be nonsmooth. In image reconstruction, the  $\phi$  term corresponds to total variation smoothing and/or L1 regularization term. The least square term  $\frac{1}{2}\|\mathcal{F}_p Su - f\|^2$  is the fidelity term. In our application,  $f$  represents undersampled data from a partially parallel imaging (PPI) system. The proposed algorithm is a generalization of the Bregman operator splitting algorithm with variable stepsize (BOSVS) in which the previous Barzilai-Borwein (BB) step is replaced by a cyclic BB (CBB) step, and an L1 term  $\Psi$  is added to the energy function. Experimental results on clinical partially parallel imaging data are given.

**Index Terms**— Image reconstruction, optimization, magnetic resonance imaging, sensitivity encoding

## 1. INTRODUCTION

Partially parallel magnetic resonance imaging plays an important role in medical imaging [1]–[4]. This uses multiple radio-frequency receiver surface coils to acquire k-space data simultaneously. To accelerate the imaging, the k-space data is partially sampled. Partial data acquisition reduces scan time by increasing the spacing between regular subsequent read-out lines. However, this reduction in the number of recorded Fourier components leads to aliasing artifacts in images [5]. Sensitivity encoding (SENSE) is one of the most common methods in partially parallel imaging (PPI) systems for removing aliasing artifacts and reconstructing images with high quality. It uses information for the coil sensitivities to separate aliased pixels produced from an undersampled k-space.

\*THIS RESEARCH WAS PARTLY SUPPORTED BY NATIONAL SCIENCE FOUNDATION GRANT 1115568, AND BY OFFICE OF NAVAL RESEARCH GRANT N00014-11-1-0068.

## 1.1. Mathematical formulation of SENSE

The fundamental equations of SENSE for a PPI system consisting of  $L$  coil arrays are as follows:

$$\mathcal{F}_p S_l u - f_l = 0, \quad l = 1, \dots, L$$

Here,  $u \in \mathbb{C}^N$  is the reconstructed image,  $S_l$  is a diagonal sensitivity map for channel  $l$ ,  $f_l$  is the undersampled data for the underlying image  $u$ ,  $\mathcal{F}_p$  is the undersampled Fourier transform defined by  $\mathcal{F}_p = P\mathcal{F}$  where  $P$  is a mask (binary matrix) and  $\mathcal{F}$  is a Fourier transform matrix.

The image  $u$  can be recovered from the undersampled data in a PPI system by solving the following least square problem:

$$\min_u \|\mathcal{F}_p Su - f\|^2,$$

where  $S = [S_1; \dots; S_N]$  and  $f = [f_1; \dots; f_N]$ . Here  $[X; Y]$  denotes the matrix obtained by stacking the matrix  $X$  above matrix  $Y$ , and  $\|\cdot\|$  denotes the Euclidean norm for a vector and the Frobenius norm for a matrix. In sensitivity encoding, samples are either along a regular Cartesian k-space grid or non-Cartesian k-space trajectory and the underlying inversion can be ill-conditioned. To cope with the ill conditioning, regularization terms are often incorporated in the minimization.

In this paper, we propose a new algorithm for reconstructing an image  $u$  from  $f$  by solving the following optimization problem:

$$\min_u \phi(Bu) + \frac{1}{2}\|\mathcal{F}_p Su - f\|^2, \quad (1)$$

where  $\phi(\cdot)$  is convex and real valued function but possibly nondifferentiable,  $B \in \mathbb{C}^{n \times N \times N}$ . The problem (1) has received considerable attention due to its application in signal and image processing and in compressed sensing, see [1]–[11].

## 1.2. Previous Works

In this section, we introduce some algorithms based on splitting. Let us introduce an auxiliary variable  $w = [w_1, \dots, w_N]$ , where  $w_i \in \mathbb{R}^2$  for  $i = 1, \dots, N$ . We rewrite problem (1) as:

$$\min_{u,w} \phi(w) + \frac{1}{2}\|\mathcal{F}_p Su - f\|^2, \quad s.t. \quad w = Bu. \quad (2)$$

Zhang, Burger and Osher in [3] introduced the following Bregman operator splitting (BOS) algorithm:

Initialize parameters  $\rho > 0$ , starting guesses  $u^0$ ,  $w^0$  and  $x^0$ , and set  $\delta_k = \delta > 0$  fixed for all  $k$ . Set  $k = 0$ .

**While** “not converged,” **Do**

Step 1.

$$u^{k+1} = \operatorname{argmin}_u \left\{ \delta_k \|u - u^k + \delta_k^{-1} S^T \mathcal{F}_p^T (\mathcal{F}_p S u^k - f)\|^2 + \rho \|Bu - w^k - \rho^{-1} x^k\|^2 \right\}.$$

Step 2.  $w^{k+1} = \operatorname{argmin}_w \left\{ \phi(w) + \frac{\rho}{2} \|w - Bu^{k+1} - \rho^{-1} x^k\|^2 \right\}$ .

Step 3.  $x^{k+1} = x^k - \rho(w^{k+1} - Bu^{k+1})$ .

Step 4.  $k = k + 1$ .

**End Do**

Here  $x^k$  is the approximation to the Lagrange multiplier associated with the constraint  $w = Bu$ . Step 1 minimizes the augmented Lagrangian with respect to the image  $u$ . Step 2 minimizes the augmented Lagrangian over the auxiliary variable  $w$ , and Step 3 is the first-order update of the multiplier. Numerical results on magnetic resonance imaging have shown that this algorithm decreases the cost function of problem (2) monotonically. Moreover, Theorem 4.2 in [3] proves convergence when  $\delta$  is strictly greater than  $\|S^T \mathcal{F}_p^T \mathcal{F}_p S\|$ .

This split Bregman algorithm with the Brazilai-Borwein stepsize (SBB) introduced in [1] takes

$$\delta_k = \frac{\|\mathcal{F}_p S(u^k - u^{k-1})\|^2}{\|u^k - u^{k-1}\|^2}.$$

Numerical experiments for the SBB algorithm on magnetic resonance imaging demonstrated that it was faster than the BOS algorithm. However, there was no convergence analysis for the SBB algorithm.

The recently proposed Bregman operator splitting with variable stepsize (BOSVS) algorithm [4] often performs better than both BOS and SBB. The algorithm is as follows:

Initialize parameters  $\tau > 1$  and  $\eta > 1$ ,  $\delta_{\min} > 0$ ,  $\sigma \in (0, 1)$ , starting guesses  $u^0$ ,  $w^0$ ,  $x^0$ . Set  $k = 0$ .

**While** “not converged,” **Do**

Step 1. Choose  $\hat{\delta}_k = \max\{\delta_{\min}, \frac{\|\mathcal{F}_p S(u^k - u^{k-1})\|^2}{\|u^k - u^{k-1}\|^2}\}$ .

Step 2. Update  $\delta_k = \eta^j \hat{\delta}_k$  where  $j \geq 0$  is the smallest integer such that

$$\sigma \delta_k \|u^{k+1} - u^k\|^2 \geq \|\mathcal{F}_p S(u^{k+1} - u^k)\|^2,$$

$$u^{k+1} = \operatorname{argmin}_u \left\{ \delta_k \|u - u^k + \delta_k^{-1} S^T \mathcal{F}_p^T (\mathcal{F}_p S u^k - f)\|^2 + \rho \|Bu - w^k - \rho^{-1} x^k\|^2 \right\}.$$

Step 3. If  $\delta_k > \delta_{k-1}$ , then  $\delta_{\min}$  is replaced by  $\tau \delta_{\min}$ .

Step 4.  $w^{k+1} = \operatorname{argmin}_w \left\{ \phi(w) + \frac{\rho}{2} \|w - Bu^{k+1} - \rho^{-1} x^k\|^2 \right\}$ .

Step 5.  $x^{k+1} = x^k - \rho(w^{k+1} - Bu^{k+1})$ .

Step 6.  $k = k + 1$ .

**End Do.**

Theorem 3.5 in [4] shows that the sequence generated by BOSVS globally converges to a solution of (1) and (2).

The main contribution of this paper is to propose a new algorithm for solving (1). This algorithm is an improved version of the BOSVS algorithm, which replaces the BB step of BOSVS with a cyclic step.

## 2. CYCLIC BREGMAN OPERATOR SPLITTING WITH VARIABLE STEPSIZE ALGORITHM

The cyclic BOSVS algorithm reads as follows:

Initialize parameter  $m > 1$ ,  $\tau > 1$  and  $\eta > 1$ ,  $\delta_{\min} > 0$ ,  $\sigma \in (0, 1)$  and starting guess  $u^0$ ,  $w^0$  and  $x^0$ . Set  $i = 0$ .

**While** “not converged”, **Do**

Step 1. Choose  $\hat{\delta}_i = \max\{\delta_{\min}, \frac{\|\mathcal{F}_p S(u^i - u^{i-1})\|^2}{\|u^i - u^{i-1}\|^2}\}$ .

Step 2. **For**  $k = i : i + m - 1$  **repeat**

Step 2.1. Update  $\delta_k = \eta^j \hat{\delta}_i$  where  $j \geq 0$  is the smallest integer such that

$$\sigma \delta_k \|u^{k+1} - u^k\|^2 \geq \|\mathcal{F}_p S(u^{k+1} - u^k)\|^2,$$

$$u^{k+1} = \operatorname{argmin}_u \left\{ \delta_k \|u - u^k + \delta_k^{-1} S^T \mathcal{F}_p^T (\mathcal{F}_p S u^k - f)\|^2 + \rho \|Bu - w^k - \rho^{-1} x^k\|^2 \right\}.$$

Step 2.2.  $w^{k+1} = \operatorname{argmin}_w \left\{ \phi(w) + \frac{\rho}{2} \|w - Bu^{k+1} - \rho^{-1} x^k\|^2 \right\}$ .

Step 2.3.  $x^{k+1} = x^k - \rho(w^{k+1} - Bu^{k+1})$ .

**End For**

Step 3. If  $\delta_k > \delta_{k-1}$  for some  $k$ , then  $\delta_{\min}$  is replaced by  $\tau \delta_{\min}$ .

Step 4. Set  $i = i + m$ .

**End Do**

Theorem 2.1. *If there exists a solution of (2), then the sequence  $(u^k, w^k, x^k)$  generated by cyclic BOSVS approaches a point  $(u^*, w^*, x^*)$  where the first-order optimality conditions for (2) are satisfied. Moreover,  $(u^*, w^*)$  is a solution of (2) and  $u^*$  is a solution of (1).*

The proof of Theorem 2.1 has the same structure as the proof of Theorem 3.5 in [4]. Notice that the  $u$ -subproblem in Step 2 is differentiable. Hence, by first order optimality condition, we have

$$(\delta_k I + \rho B^T B) u^{k+1} = \mathcal{R}^k,$$

where

$$\mathcal{R}^k = (\delta_k - S^T \mathcal{F}_p^T \mathcal{F}_p S) u^k + \rho B^T (w^k - \rho^{-1} x^k) + S^T \mathcal{F}_p^T f.$$

Let  $\bar{\Delta} = \mathcal{F} B^T B \mathcal{F}^T$  be a diagonalization of  $B^T B$  using the Fourier transform  $\mathcal{F}$ . Hence,

$$u^{k+1} = \mathcal{F}^T (\delta_k I + \rho \bar{\Delta}) \mathcal{F} \mathcal{R}^k.$$

The solution of  $w$ -subproblem depends on the form of  $\phi$ .

Recovering MR images from undersampled Fourier measurement  $f$  can usually be obtained by taking  $\phi(Bu)$  of the form:

$$\phi(Bu) = \beta_1 \|Du\|_1 + \beta_2 \|\Psi u\|_1, \quad (3)$$

where  $\beta_1, \beta_2 \geq 0$ . The matrix  $\Psi \in \mathbb{C}^{N \times N}$  is unitary and  $D \in \mathbb{C}^{2 \times N \times N}$  where  $Du$  is a  $2 \times N$  matrix with  $(Du)_i$  the discrete gradient (finite differences along the coordinate directions) of  $u$  at the  $i$ -th pixel in the image, and  $\|Du\|_1 = \sum_{i=1}^N \|(Du)_i\|_2$ .

Let us define

$$B = \begin{pmatrix} D \\ \Psi \end{pmatrix}, \quad w = \begin{pmatrix} \bar{w} \\ \hat{w} \end{pmatrix} = \begin{pmatrix} Du \\ \Psi u \end{pmatrix}, \quad x = \begin{pmatrix} \bar{x} \\ \hat{x} \end{pmatrix}$$

where  $B \in \mathbb{C}^{3 \times N \times N}$ ,  $\bar{w}$  and  $\bar{x} \in \mathbb{C}^{2 \times N}$ ,  $\hat{w}$  and  $\hat{x} \in \mathbb{C}^N$ . With this choice for  $B$  and  $\phi$ , Step 2.2. in cyclic BOSVS become:

$$\bar{w}^{k+1} = \underset{\bar{w}}{\operatorname{argmin}} \{ \beta_1 \|\bar{w}\|_1 + \frac{\rho}{2} \|\bar{w} - Du^{k+1} - \rho^{-1} \bar{x}^k\|^2 \},$$

$$\hat{w}^{k+1} = \underset{\hat{w}}{\operatorname{argmin}} \{ \beta_2 \|\hat{w}\|_1 + \frac{\rho}{2} \|\hat{w} - \Psi u^{k+1} - \rho^{-1} \hat{x}^k\|^2 \}.$$

Here, the solution of  $\bar{w}$ -subproblem and  $\hat{w}$ -subproblem can be obtained by the soft shrinkage operator [11]. For  $i = 1, \dots, N$ :

$$\bar{w}_i^{k+1} = \mathcal{S}_1 \{ (Du^{k+1} + \rho^{-1} \bar{x}^k)_i, \beta_1 \},$$

$$\hat{w}_i^{k+1} = \mathcal{S}_2 \{ (\Psi u^{k+1} + \rho^{-1} \hat{x}^k)_i, \beta_2 \},$$

where for any  $\bar{t} \in \mathbb{C}^2$ ,  $\hat{t} \in \mathbb{C}$  and  $\beta \in \mathbb{R}$ :

$$\mathcal{S}_1(\bar{t}, \beta) := \frac{t}{\|\bar{t}\|_2} \max\{\|\bar{t}\|_2 - \beta, 0\},$$

$$\mathcal{S}_2(\hat{t}, \beta) := \frac{\hat{t}}{|\hat{t}|} \max\{|\hat{t}| - \beta, 0\},$$

with the conventions  $0/0 = 0$ .

### 3. EXPERIMENTAL RESULTS

This section tests the effectiveness of the cyclic BOSVS to recover images on a PPI system, and compares the results to three different algorithms: BOS, SBB and BOSVS. For this, we use two data sets denoted data1 and data2, obtained from commercially available eight-channel PPI systems, i.e.  $L = 8$ . The data acquisition parameters for these two data sets are given in Table 1. The mask and reference image for data1 are in Figures 1(a) and (b), while the corresponding mask and image for data2 are in Figures 1(c) and (d). The artificially undersampled data  $f_i := P\mathcal{F}(s_i \odot u) + n_i$ , where  $n_i$  is complex valued white Gaussian noise with standard deviation  $\bar{\sigma} = 0.7 \times 10^{-3}$  for both of the real and imaginary parts.

**Table 1.** The data acquisition parameters for data1 and data2.

Parameters	data1	data2
TR	3060 ms	3000 ms
TE	126 ms	85 ms
FOV	220 mm <sup>2</sup>	205 mm <sup>2</sup>
Size $\times 8$	512 $\times$ 512 $\times$ 8	500 $\times$ 512 $\times$ 8
ST	5mm	5mm
FA	90 <sup>o</sup>	90 <sup>o</sup>

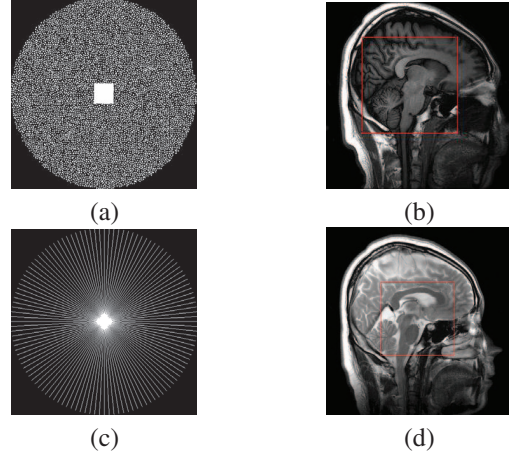


**Fig. 1.** (a) Pseudo random mask with reduction factor 4. (b) The reference image in data1. (c) Radial mask with reduction factor 6. (d) The reference image in data2.

In our numerical and experimental results, we solve the optimization problem (2) with  $\phi$  of the form (3) where  $\beta_1 = 10^{-4}$  and  $\beta_2 = 0$ . The parameter values that we used were  $m = 7$ ,  $\rho = 10^{-2}$ ,  $\tau = 2$ ,  $\delta_{\min} = 0.001$ ,  $\eta = 3$  and  $\sigma = 0.99999$ . The reconstructed images using the cyclic BOSVS algorithm applying to data1 and data2 are shown in Fig. 2. In this section we use 25 CPU (sec.) time to recover the image from data1 and 90 CPU (sec.) to recover the image from data2. Table 2 shows the comparison of the corresponding objective function values. A plot of cost function value versus CPU time is also given in Fig. 3. Notice that cyclic BOSVS achieves the best objective function value for the given allotment of CPU time.

**Table 2.** Comparison of the final objective function value shown in Figure 3.

	BOS	SBB	BOSVS	cyclic BOSVS
Obj-data1	0.5410	0.5275	0.5045	0.5040
Obj-data2	1.9361	1.9177	1.8247	1.8197

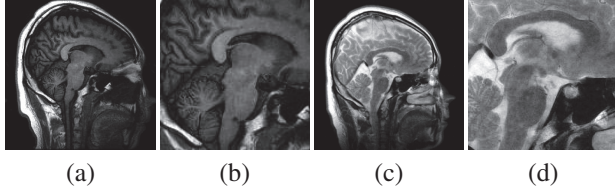


**Fig. 2.** Left to right: (a) image reconstruction by the cyclic BOSVS algorithm using data1. (b) Magnification of the reconstructed image. (c) Image reconstruction using the cyclic BOSVS algorithm using data2. (d) Magnification of the reconstructed image.

#### 4. CONCLUDING REMARKS

In this paper, we proposed an improvement version of the Bregman operator splitting algorithm with variable stepsize. The algorithm uses the cyclic BB step instead of the BB step used in BOSVS. Comparisons were made between BOSVS [4], SBB [1] and BOS [3] using partially parallel magnetic resonance image reconstruction problems. The cyclic BOSVS algorithm provided high quality image reconstructions relatively efficiently.

#### 5. REFERENCES

[1] X. Ye, Y. Chen, and F. Huang, "Computational acceleration for MR image reconstruction in partially parallel imaging," *IEEE Trans. Med. Imaging*, vol. 30, pp. 1055–1063, 2011.

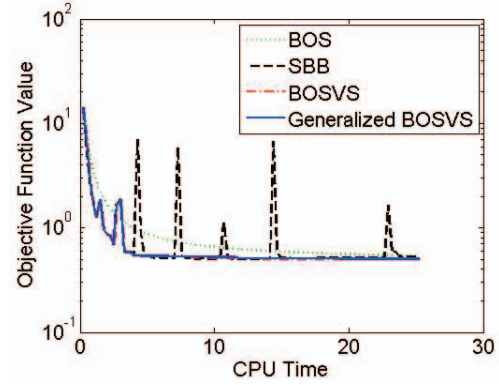
[2] Y. Chen, W. W. Hager, F. Huang, D. T. Phan, X. Ye, and Wotao Yin, "A fast algorithm for image reconstruction with application to partially parallel MR imaging," *SIAM J. Imaging Sci.*, vol. 5, 2012.

[3] Xiaoqun Zhang, Martin Burger, and Stanley Osher, "A unified primal-dual algorithm framework based on Bregman iteration," *J. Sci. Comput.*, vol. 46, pp. 20–46, 2011.

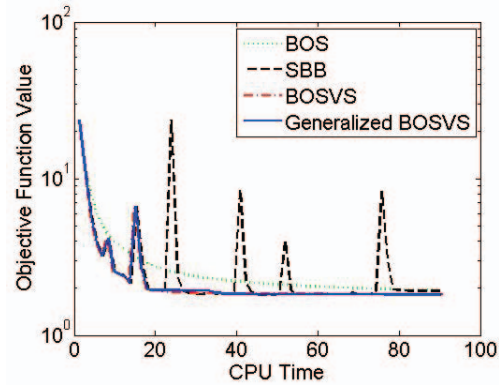
[4] Y. Chen, W. W. Hager, M. Yashtini, and X. Ye, "Bregman operator splitting with variable stepsize for total variation image reconstruction," *Comput. Optim. Appl.*, 2012, submitted.

[5] K. Block, M. Uecker, and J. Frahm, "Undersampled radial MRI with multiple coils: Iterative image reconstruction using a total variation constraint," *Magn. Reson. Med.*, vol. 57, pp. 1086–1098, 2007.

[6] K.P. Pruessmann, M. Weiger, M.B. Scheidegger, and P. Boesiger, "SENSE: Sensitivity encoding for fast MRI," *Magn. Reson. Med.*, vol. 42, pp. 952–962, 1999.



(a)



(b)

**Fig. 3.** Comparison of objective function versus CPU time. (a) using data1, (b) using data2.

[7] S. Ramani and J. A. Fessler, "Parallel MR image reconstruction using augmented lagrangian methods," *IEEE Trans. Med. Imag.*, vol. 30, pp. 1165–1195, 2011.

[8] T. Goldstein and S. Osher, "The split Bregman method for L1 regularized problems," *SIAM J. Imag. Sci.*, vol. 2, pp. 323–343, 2009.

[9] J. Yang, Y. Zhang, and W. Yin, "A fast alternating direction method for TVL1-L2 signal reconstruction from partial Fourier data," *IEEE J. Selected Topics Signal Process.*, vol. 4, pp. 288–297, 2010.

[10] X. Zhang, M. Burger, X. Bresson, and S. Osher, "Bregmanized nonlocal regularization for deconvolution and sparse reconstruction," *SIAM J. Imaging Sci.*, vol. 3, pp. 253–276, 2011.

[11] Y. Wang, J. Yang, W. Yin, and Y. Zhang, "A new alternating minimization algorithm for total variation image reconstruction," *SIAM J. Imag. Sci.*, vol. 1, no. 3, pp. 248–272, 2008.